

Scaling Laws for Mode Lockings in Circle Maps

Predrag Cvitanović*

Laboratory of Atomic and Solid State Physics, Cornell University, Ithaca, NY 14853, USA

Boris Shraiman

The James Franck Institute, University of Chicago, Chicago IL 60637, USA

and

Bo Söderberg**

Nordita, Blegdamsvej 17, DK-2100 Copenhagen Ø. Denmark

Received April 22, 1985; accepted May 17, 1985

Abstract

The self-similar structure of mode lockings for circle maps is studied by means of the associated Farey trees. We investigate numerically several classes of scaling relations implicit in the Farey organization of mode lockings and discuss the extent to which they lead to universal scaling laws.

1. Introduction

The discovery of the universality for period-doublings in one-dimensional iterations [1], [2] has prompted a search for universal scalings in other low dimensional dynamical systems (the theory and the experimental observations of period doublings are reviewed in refs. [3–7]).

One class of such problems in which the universality ideas have had some success are the transitions to chaos for diffeomorphisms on the circle (circle maps). Maps of this type model a variety of physical systems: we refer the reader to refs. [8], [9] for a discussion of the physical applications of circle maps.

A prototype mapping of this type is the *sine* map

$$x_{n+1} = x_n + \Omega - k/(2\pi) \sin(2\pi x_n) \pmod{1} \quad (1.1)$$

The circle maps fall into three classes. If the map is monotonically increasing (k smaller than 1 in (1.1)), it is called *subcritical*. For subcritical maps the asymptotic scaling laws turn out to be trivial: they are given by the shift map ($k = 0$ in (1.1)) scalings. For the *shift* map

$$x_{n+1} = x_n + \Omega \pmod{1} \quad (1.2)$$

the parameter Ω is also the winding number of the mapping. Mode lockings correspond to rational windings, so the problem of organizing subcritical mode lockings reduces to the problem of organizing rationals on the unit interval. There are various ways of doing this: we argue that the natural organization is given by the Farey tree (section 3).

If the map is marginally invertible, i.e. if it has inflection points with zero slope ($k = 1$ in (1.1)), it is called *critical*. This is the physically interesting class, as the dynamical systems

modelled by circle maps in this case exhibit transitions to chaos already on a two-torus.

Finally, if the map is non-invertible (k larger than 1 in (1.1)), it is called *supercritical*. The bifurcation structure of this regime is extremely rich. Beyond mode lockings and period doublings there are infinitely many families of infinite sequences of bifurcations which tend to universal limits.

In this paper we concentrate on the critical case. The trivial subcritical case is nothing but easy number theory (the Farey tree, binary trees, continued fractions), which we use as a guide to organization of the non-trivial critical case. Our goal is to formulate universal scaling laws which characterize the critical case, and which have a chance of being experimentally accessible. By saying that a scaling law for mode lockings is “universal” we mean that it should apply to any critical circle map within the given universality class. The *universality class* of a critical map depends on the power of inflection. The generic, physically interesting case corresponds to the cubic inflection (for $k = 1$ and small x , (1.1) is cubic in x). All our calculations are done for the critical maps with cubic inflections.

The first example of a universal scaling for the critical circle maps was discovered in a study of mappings with golden mean winding number [10–12]. While appealing theoretically, the golden mean universality describes a very small region of the total parameter space and is difficult to measure experimentally.

The next example of universality was discovered by M. H. Jensen *et al.* [13]. They have observed that the fractal dimension of the parameter values corresponding to the irrational windings is (numerically) universal, $D = 0.87 \dots$. Unlike the golden mean universality, this is a global statement about the whole parameter range, and D is easily extracted from experimental data.

Clearly, there is much more universality to be mined from circle maps. In this paper, motivated by the desire to extract as much scaling information as possible, and thus have a stronger hand in confronting the experiments, we propose and investigate numerically a number of different scaling laws which characterize *all* mode lockings.

2. Circle maps

A circle map is a mapping of a circle onto itself of form

* Permanent address: Theoretical Physics, Chalmers University, S-412 96 Goteborg, Sweden.

** Address until 1 July 1985: Centre de Physique Théorique CNRS, Luminy, F-13288 Marseille, France.

$$\begin{aligned}
 x \rightarrow x' &= f(x) \pmod{1} \\
 f(x+1) &= f(x) + 1
 \end{aligned}
 \tag{2.1}$$

$f(x)$ is assumed to be continuous, have continuous first derivative, and in addition have continuous second derivative at the inflection points. One example of a circle map is the sine mapping (1.1). Another example of such map is a (piecewise) cubic map

$$\begin{aligned}
 x_{n+1} &= \Omega + 4x_n^3 & 0 \leq x_n < 1/2 \\
 &= \Omega + 1 + 4(x_n - 1)^3 & 1/2 \leq x_n < 1
 \end{aligned}
 \tag{2.2}$$

The winding number

$$\omega = \lim_{n \rightarrow \infty} (f^n(x) - x)/n
 \tag{2.3}$$

describes the average rotation per iteration. For invertible maps and rational winding numbers, $\omega = P/Q$, the asymptotic iterates of the map converge to a unique Q -cycle attractor

$$f^Q(x_i) = x_i + P \quad i = 0, 1, 2, \dots, Q - 1
 \tag{2.4}$$

where x_i is the i th cycle point.

For any rational winding number, there is a finite interval of parameter values for which the iterates of the circle map are attracted to the P/Q cycle. We call this interval the *stability interval* of the P/Q cycle. The stability of the P/Q cycle is defined as

$$S = \frac{\partial X_Q}{\partial X_0} = f'(x_0)f'(x_1) \dots f'(x_{Q-1})
 \tag{2.5}$$

For a stable cycle, $|S|$ lies between 0 (the superstable value, the center of the stability interval) and 1 (the ends of the stability interval). A critical map has a superstable P/Q cycle for any rational P/Q , as the stability of any cycle that includes the inflection point equals zero.

For the shift map ($k = 0$), the stability intervals are actually points. As the “non-linearity” parameter k increases, they become wider, and for the critical maps ($k = 1$) they fill out the whole interval [13]. A plot of winding number ω as a function of the shift parameter Ω is a convenient way of representing the mode-locking structure of circle maps. It yields a monotonic “devil’s staircase” (see ref. [13], for example) whose self-similar structure we wish to unravel here.

We compute the stability intervals by the method due to J. Myrheim [14]. This is a two-dimensional Newton–Raphson method which determines Ω and x_0 required for a P/Q cycle (2.4) of given stability (2.5). The initial guess for the value of Ω corresponding to the superstable cycle is easily obtained by halving Ω intervals, as x_Q is a monotonic function of Ω . The stability (2.5) as a function of Ω is roughly an ellipse whose width is well estimated by its curvature

$$\Delta_{P/Q}^{\text{curv}} = \left. \frac{d^2}{d\Omega^2} \frac{\partial X_Q}{\partial X_0} \right|_{\Omega = \Omega_{\text{SS}}}
 \tag{2.6}$$

at the superstable (or if $k < 1$, the maximally attractive) point. This width is then used to start the Newton–Raphson iteration for determining the ends of the stability interval. The curvature (2.6) is an interesting object in itself, as it provides a local measure of the scale of the mode-locking intervals.

We expect universal scalings, because mode-lockings possess rich self-similarity structure. Essentially, a metric self-similarity

will arise because iterates of critical maps are themselves critical, i.e. they also have cubic inflection points. This situation is reminiscent of period-doubling universality, where iterates of quadratic polynomials are themselves locally quadratic, and where this local self-similar structure leads to the universal scaling laws.

3. Farey trees

The self-similar structure of the devil’s staircase [13], suggests a systematic way of separating the mode lockings of a circle map into a hierarchy of levels.

Intuitively, the longer the cycle, the finer the tuning of parameter Ω required to attain it. For example, we will show in section 7 that the size of the stability interval corresponding to $1/Q$ -cycle is of order Q^{-3} . The crucial observation is that roughly halfway between any two large stability intervals (such as $1/2$ and $1/3$) there is the next largest stability interval (such as $2/5$). Of all the rationals in this range of winding number values we are interested in the one with the smallest denominator. Hence we need an interpolation scheme which organizes rational numbers P/Q into self-similar levels of increasing cycle lengths Q . Such scheme is provided by Farey numbers [15], [16].

The Farey mediant [17], [18] interpolates between two rationals,

$$P/Q \oplus P'/Q' = (P + P')/(Q + Q'),
 \tag{3.1}$$

yielding the fraction with the smallest denominator lying between P/Q and P'/Q' . That the Farey composition describes the mode-lockings of not only the trivial shift map (1.2), but also the mode-lockings of the subcritical and critical circle maps, follows from their monotonicity. For the nontrivial maps the $Q + Q'$ cycle can be found in the following manner. Start with a fake $(P + P')/(Q + Q')$ cycle which consists of Q iterations of the map corresponding to the superstable P/Q cycle, followed by Q' iterations of the map corresponding to the superstable P'/Q' cycle:

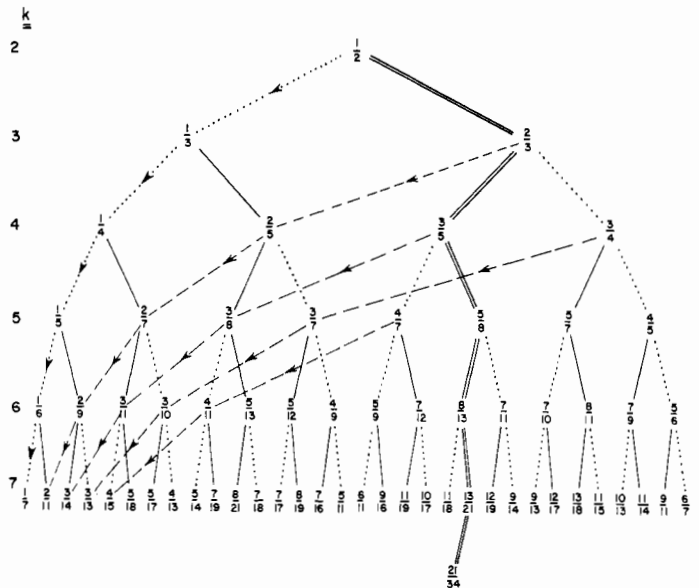


Fig. 1. The Farey tree. The double line indicates the Fibonacci sequence of rational approximations to the golden mean. The dashed lines are sequences of approximations to 0/1 of form P/Q , P fixed, Q large.

$$f_{\Omega_{P/Q}}^Q(f_{\Omega_{P'/Q'}}^{Q'}(0)) = P + P' \tag{3.2}$$

$$P/Q < P'/Q'$$

If we increase $\Omega_{P/Q}$, the Q th iterate overshoots completing the Q -cycle by a positive amount (as the map is assumed monotone); The composed map can still have a $Q + Q'$ cycle if we compensate for this overshoot by decrementing $\Omega_{P'/Q'}$. We can repeat this procedure until the two parameter values coincide. Hence the parameter interval between P/Q and P'/Q' cycles always contains the $(P + P')/(Q + Q')$ cycle.

The *Farey tree* is obtained by starting with the ends of the unit interval written as $0/1$ and $1/1$, and interpolating by means of Farey mediants. The first level of the Farey tree is $1/2$, the second $1/3, 2/3$, the third $1/4, 2/5, 3/5, 3/4$ and so forth, see Fig. 1.

The following alternative construction of the Farey tree makes the self-similarities more explicit. Replace each Farey number by its continued fraction representation $P/Q = [j, k, l, \dots, m]$,

$$[j, k, l, \dots, m] = \frac{1}{j + \frac{1}{k + \frac{1}{l + \frac{1}{\dots + \frac{1}{m}}}}} \tag{3.3}$$

with j, k, l, \dots, m positive integers. Clearly

$$[\dots, m, 1] = [\dots, m + 1]. \tag{3.4}$$

The *level* of a Farey number is given by the sum of coefficients of its continued fraction expansion. The next level of the Farey tree is obtained by replacing the “last 1” in the continued fraction by either 2 or $1/2$:

$$[j, k, l, \dots, m] \begin{cases} \text{---} [j, k, l, \dots, m + 1] \\ \text{---} [j, k, l, \dots, m - 1, 2] \end{cases} \tag{3.5}$$

The resulting Farey tree is given in Fig. 2. The continued fraction representation shows explicitly that each branch of the Farey tree is similar to the entire tree, and suggests scaling laws for the associated mode lockings.

It is clear that sequences converging to different rational or irrational numbers, such as the $1/N$ approximations to $0/1$, Fig. 1, and the $N/(2N + 1)$ approximations to $1/2$, Fig. 3, are

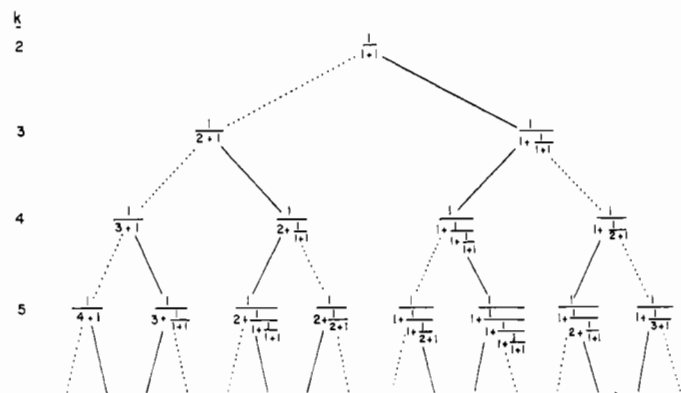


Fig. 2. A continued fraction representation of the Farey tree. The dotted and the full lines indicate substitutions by 2 and $1/2$, respectively.

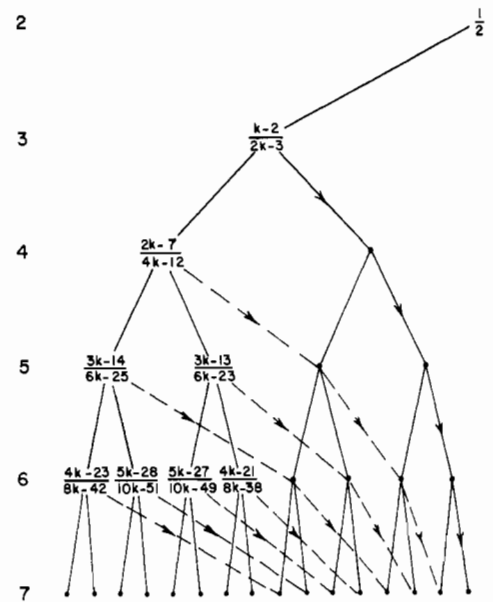


Fig. 3. Sequences of approximations to $1/2$ of form $1/(2 + M/N)$.

similar to each other, and that implicit in the Farey tree structure are scaling laws that relate mode-locking intervals. In order to describe these scalings more precisely, we need to first discuss the rationals on the unit interval in more detail.

4. Operators on the rationals

In this section we define a few elementary operations which implement various symmetries of the Farey tree, and are therefore useful in describing the scalings of the associated mode-locking intervals.

The most trivial symmetry of the Farey tree is the replacement $\omega \rightarrow 1 - \omega$, which flips the Farey tree around $1/2$, its root. In terms of continued fractions, this is given by

$$1 - \omega = \begin{cases} [1, n_1 - 1, n_2, n_3, \dots] & \text{if } n_1 > 1 \\ [n_2 + 1, n_3, \dots] & \text{if } n_1 = 1 \end{cases} \tag{4.1}$$

Clearly ω and its flip partner $1 - \omega$ belong to the same level of the Farey tree.

By the Farey rule (3.1) each rational is a daughter of two “parents”. We shall refer to the parent on the level immediately above the daughter as the “mother”, and to the more distant parent as the “father”. If we take all Farey numbers up to a given level and order them monotonically, then the two successive Farey numbers $P/Q, P'/Q'$ satisfy

$$P'/Q' - P/Q = 1/Q'Q \tag{4.2}$$

Any two “sisters” in (3.5) satisfy

$$P'/Q' - P/Q = 3/Q'Q \tag{4.3}$$

The “left parent” of a rational P/Q on the unit interval is given by

$$L\omega = P'/Q' \tag{4.4}$$

where P' and Q' are determined by (4.2):

$$PQ' = P'Q + 1, \quad 0 < Q' < Q$$

The continued fraction rule for determining the left parent follows from (3.5):

$$L[n_1, \dots, n_{k-1}, n_k] = \begin{cases} [n_1, \dots, n_{k-1}] & \text{if } k \text{ odd} \\ [n_1, \dots, n_{k-1}, n_k - 1] & \text{if } k \text{ even} \end{cases} \quad [n, x] [x] = [nx + 1] \quad (4.14)$$

$$(4.5)$$

If $n_k - 1 = 1$, replace $[\dots, n_{k-1}, 1]$ by $[\dots, n_{k-1} + 1]$.

For example (see Fig. 1), the left parent of $5/14 = [2, 1, 4]$ is $1/3 = [3]$, and the left parent of $9/14 = [1, 1, 1, 4]$ is $7/11 = [1, 1, 1, 3]$.

The dual of a rational $\omega = P/Q$ on the unit interval is defined by

$$D\omega = Q'/Q \quad (4.6)$$

where Q' is the denominator of the left parent, or, equivalently, the mod Q inverse of P :

$$PQ' = 1 \pmod{Q}, \quad 0 < Q' < Q$$

The continued fraction of the dual is obtained by reversing the continued fraction of ω :

$$D[n_1, n_2, \dots, n_k] = \begin{cases} [n_k, \dots, n_2, n_1] & \text{if } k \text{ odd} \\ [1, n_k - 1, \dots, n_1] & \text{if } k \text{ even} \end{cases} \quad (4.7)$$

If $n_1 = 1$, replace $[\dots, n_2, 1]$ by $[\dots, n_2 + 1]$. For $\omega = 0/1$, $D\omega = \omega$.

For example (see Fig. 1), the dual of $5/14 = [2, 1, 4]$ is $3/14 = [4, 1, 2]$, and the dual of $9/14 = [1, 1, 1, 4]$ is $11/14 = [1, 3, 1, 2]$.

The dual operation is idempotent and it commutes with the flip (4.1):

$$DD = 1 \quad (4.8)$$

$$D(1 - \omega) = 1 - D\omega$$

The dual $D\omega$ belongs to the same Farey level as ω .

The Gauss transformation is defined as

$$G\omega = \{1/\omega\}$$

where $\{ \}$ stands for the fractional part $\{x\} = x - \text{Int}(x)$. The dual equivalent of the left parent is defined as

$$T = DLD \quad (4.9)$$

and it can be shown to be identical to $T = 1 - G$.

The continued fraction rule for the operation T is given by

$$T[n_1, n_2, n_3, \dots] = \begin{cases} [1, n_2 - 1, n_3, \dots] & \text{if } n_2 > 1 \\ [n_3 + 1, \dots] & \text{if } n_2 = 1 \end{cases} \quad (4.10)$$

For example (see Fig. 1), $T(5/14) = T[2, 1, 4]$ is $1/5 = [5] = \{-14/5\}$, and $T(7/16) = T[2, 3, 2]$ is $5/7 = [1, 2, 2] = \{-16/7\}$.

The last s integer entries in the continued fraction $[n_1, n_2, \dots, n_k, m_s, m_{s-1}, \dots, m_1]$ can be replaced by the corresponding rational x :

$$\omega(x) = [n_1, n_2, \dots, n_k, 1/x] \quad (4.11)$$

$$x = [m_s, m_{s-1}, \dots, m_1]$$

By the definition of the continued fraction (3.3)

$$[\dots, m, n, 1/x] = [\dots, m, n + x] \quad (4.12)$$

We can evaluate $\omega'(0)$ recursively using identities

$$\frac{d}{dx} [m, n, \dots, x] = -[m, n, \dots, x] \frac{2d}{dx} [n, \dots, x] \quad (4.13)$$

$$[n, x] [x] = [nx + 1] \quad (4.14)$$

The result is

$$\omega'(0) = (-1)^k / Q^2 \quad (4.15)$$

and the infinitesimal neighborhood of ω is given by

$$\omega(x) = \omega + (-1)^k x / Q^2 + x^2 \omega''(0) / 2 + \dots \quad (4.16)$$

$$\omega = P/Q = [n_1, n_2, \dots, n_k] \quad (4.17)$$

5. Scaling functions

The physically interesting question about mode lockings is the question of what mode lockings are the dominant ones, and what are their relative scales. The Farey tree guides us to the answers: it organizes all mode lockings into a hierarchy of levels, and suggests scaling laws. A scaling law is a statement of self-similarity: it says that asymptotically every branch of the Farey tree resembles some other branch. In this sense there is an infinity of scaling laws. However, most of them are redundant: if we know how the scale changes from a level to the next level, we can compute the scaling connecting any two levels. Hence the main object of interest is the ratio of the local scale of a “mother” mode-locking to the local scale of a “daughter” mode locking. As every Farey number has two “parents” (3.1), it is natural to compare the scale of the daughter to the scale of either parent:

$$\sigma = \frac{\Delta(\text{daughter})}{\Delta(\text{parent})} \quad (5.1)$$

From now on we shall refer to this ratio as the *scaling function*. The scale associated with a given mode locking can be defined in a variety of ways. As each Farey number has two daughters, one can use the separation between the maximally stable (for critical circle maps, the superstable) parameter values of the two daughters as a measure of the local scale:

$$\Delta^{\text{cent}} = \Omega_d - \Omega_{d'} \quad (5.2)$$

We shall call this the *centroid* splitting. Another, experimentally more accessible measure of the scale associated with a given mode locking, is the mode-locking *interval* size, i.e. the difference between the parameter values corresponding to the left and to the right edges of the P/Q mode-locking region:

$$\Delta^{\text{int}} = \Omega_R - \Omega_L \quad (5.3)$$

A truly *local* measure of the scale associated with a super-stable cycle is the curvature (2.6). The centroid, the interval and the local scaling functions are in general *not equal*.

Our next problem is to decide what is (5.1) a function of. A glance at the Farey tree Fig. 1 reveals that at every branching there is a slow and a rapid change of scale, corresponding to the two extremes in denominator growth rates:

If we follow the tree down along the outside, dotted branches, the denominators grow *harmonically*, i.e. as N , where N is the level of the Farey tree. The corresponding mode-locking intervals decrease slowly, and the associated daughter/mother ratios tend to 1.

The other extreme is obtained by zig-zagging down the center of the tree. The successive denominators grow *geometrically*, gaining a golden mean factor at each level. The corresponding mode-locking intervals decrease by the universal Shenker’s factor [10] δ . Hence we already know that the

scaling function (5.1) is universal for at least one winding number, the golden mean. Furthermore, as this universality follows from the periodicity of the associated continued fraction expansion, we know that for any finite interval on the winding number axes there are infinitely many windings for which the scalings are of the golden mean type. Interspersed between them are winding numbers of harmonic type, so it clearly makes no sense to define the scaling function as a monotonic function of the daughter's winding number.

To discover more sensible labelings of the scaling function (5.1), we turn to the shift map (1.2). The separation of the two daughters (5.2) is given by (4.3), so the centroid scaling function for the shift map is

$$\sigma_{P'/Q'}^{\text{cent}} = \frac{\Delta_{P'/Q'}^{\text{cent}}}{\Delta_{P/Q}^{\text{cent}}} = \frac{Q'Q''}{Q'_d Q''_d} \quad (5.4)$$

All of the above Q 's can be expressed in terms of the mother-daughter pair Q, Q' :

$$\begin{aligned} Q'' &= 3Q - Q' \\ Q'_d &= 2Q' - Q \\ Q''_d &= Q + Q' \end{aligned} \quad (5.5)$$

and (5.4) becomes

$$\sigma(x) = \frac{3x - 1}{(2 - x)(1 + x)} \quad (5.6)$$

$$x = Q_{\text{mother}}/Q_{\text{daughter}}, \quad 1 > x > 1/2$$

Hence the trivial circle map suggests that the daughter scaling should be plotted as a function of the *dual* (4.6) of its rotation number [19].

The centroid scaling function (5.6) is not a particularly pretty object because the centroid splitting (5.2) is a very crude measurement of the scale of the neighborhood of P/Q . The unique *local* scale can be defined by studying the splitting between two harmonic sequences approaching P/Q : the sequence that approaches P/Q from below, with $\tilde{Q}' = Q' + NQ$, and the sequence that approaches P/Q from above, with $\tilde{Q}'' = Q'' + NQ$. In the large N limit the splitting is given by (see (40.17))

$$\Delta_{P/Q}^{(N)} = \frac{2}{N} \frac{1}{Q^2} \quad (5.7)$$

and the corresponding trivial *local* scaling functions is given by

$$\sigma(x) = x^2 \quad (5.8)$$

where $x = D\omega$ is the dual (4.6) of the daughter winding number ω .

6. The binary-labelled scaling function

The structure of the Farey tree suggests an alternative labelling of the mode-locking intervals: the *binary labeling* [20]. Assign 0 to all “slow” branches (dotted lines in Fig. 1), 1 to all “fast” branches (full lines in Fig. 1), and assign to each Farey number a binary coordinate, obtained by reading the bits starting with the corresponding branch and continuing up the tree. This has the virtue that all the numbers whose continued fractions asymptotically look like the golden mean continued fraction lie together at the end of the unit interval, while the other extreme, the harmonic sequences with denominators growing like the Farey level, lie at the beginning of the interval. We have plotted

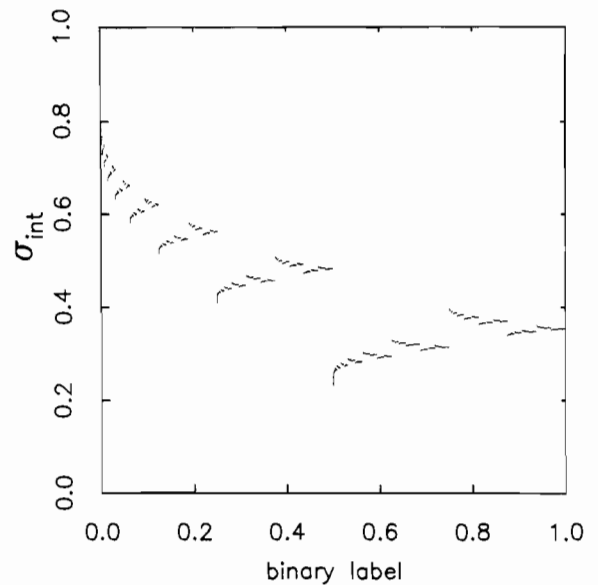


Fig. 4. The binary-labelled scaling function: ratio of daughter/mother stability intervals (5.3) is plotted as the function of daughter's binary label. The rightmost point corresponds to the golden mean winding number: there the value of the scaling function is Shenker's δ . The leftmost point corresponds to the $1/N$ harmonic sequence: there the scaling function approaches 1.

a binary-labelled scaling function in Fig. 4. A binary-labelled scaling function is discontinuous at every binary rational, and self-similar in a way that makes it resemble a flock of seagulls. This self-similar structure is solely an artifact of the binary labelling. The corresponding trivial scaling function obtained by plotting (5.8) as the function of the binary label (rather than the dual of the daughter's winding number) is visually indistinguishable from the nontrivial scaling function of Fig. 4.

Shenker's [10] δ is a statement of the self-similarity of mode lockings for the Fibonacci approximations to $(\sqrt{5} - 1)/2$, the golden mean. The binary-labelled scaling function is an extension of scaling by Shenker's δ to all mode lockings: it states that not only the sequence of Fibonacci approximations is self-similar, but that the entire neighborhood of the golden mean is self-similar. Such scaling function organizes the mode-locking intervals around the golden mean: it is an example of a scaling function which concentrates on *the geometric scaling*.

The doubling structure of the Farey tree, its binary labeling, and the resulting scaling function are strikingly reminiscent of period doublings. Indeed, they look so much like period doublings that M. J. Feigenbaum [21], following our proposal [22], has actually succeeded in turning the binary labeled Farey tree into a period-doubling dynamics (in the parameter space, this time). Shenker's δ plays here the same role that the universal scaling number α plays for period doubling, and the universality of the binary-labelled scaling function follows from the machinery developed for the period-doubling theory and the previous work on the golden mean universality [11], [12].

As the binary labelled scaling functions are discussed in detail in ref. [21], we concentrate in this paper on the dual-labelled scaling functions of type (5.8). Dual labellings result in somewhat smoother and perhaps more “natural” scaling functions. The binary- and the dual-labelled scaling functions are related by a trivial relabelling, and our numerical results are equally significant for either version.

7. Harmonic sequences

The binary labelled scaling function is a precise statement of the similarity of the successive subtrees obtained by zig-zagging down the center of the Farey tree – it is the simplest example of geometric scaling for mode lockings.

Here we turn to the other extreme: scalings for harmonic sequences, such as $1/2 \rightarrow 1/3 \rightarrow \dots \rightarrow 1/N \rightarrow 1/(N + 1)$ (or any sequence that follows a dotted line in Fig. 1). The interval between $1/(N + 1)$ and $1/N$ contains an entire Farey subtree (the first level $1/(N + 1/2)$, the second consists of $1/(N + 1/3)$, $1/(N + 2/3)$, and so on) parametrized by

$$\omega = \frac{1}{N + 1 - x}, \quad 0 < x < 1 \tag{7.1}$$

If such subtrees approach a limit for large N , we say that they exhibit *harmonic scaling*. For the trivial circle map they indeed do scale: reparametrize the shift map (1.2) by

$$\Omega = \Omega_{n+1} + (\Omega_n - \Omega_{n+1})p = \frac{1}{N + 1} + \frac{p}{N(N + 1)}. \tag{7.2}$$

The winding number (2.3) for the trivial map is

$$\omega = \frac{1}{N + 1 - x} = \frac{1}{N + 1} + \frac{x}{(N + 1 - x)(N + 1)} \tag{7.3}$$

so

$$p = \frac{N}{N + 1 - x} x = x + O(1/N) \tag{7.4}$$

For large N the Farey subtree between $1/(N + 1)$ and $1/N$ is a replica of the entire tree, rescaled by the factor N^{-2} .

A numerical analysis of the stability intervals (5.3) for the $1/N$ mode lockings shows that asymptotically

$$N^3 \Delta(1/N) \rightarrow \text{const.} \quad \text{as } N \rightarrow \infty \tag{7.5}$$

(here Δ is any of the scale indicators (5.2), (5.3) or (2.6)).

This power law behaviour can be explained by the same argument as those used in modelling of intermittency [23]. For $1/N$ cycles the value of the parameter Ω lies just above Ω_R , the right edge of the 0/1 stability interval. The corresponding circle map (2.1) almost touches the $y = x$ line, leaving only a tiny gap to x^* , the fixed point corresponding to the right edge of the 0/1 stability interval. In the neighborhood of x^* we can approximate $f(x)$ by

$$f(x) \simeq x + \epsilon^2 + a^2(x - x^*)^2 \tag{7.6}$$

$$a^2 = f''(x^*)/2, \quad \epsilon^2 = \Omega - \Omega_R$$

For small ϵ we can approximate the above iteration by a differential equation in terms of a rescaled variable $y = (x - x^*)/\epsilon$ and “time” variable $t = n\epsilon$,

$$\frac{dy}{dt} = 1 + (ay)^2 \tag{7.7}$$

with the solution $t = a^{-1} \arctan(ay)$.

The time required to pass through the trough is π/a , corresponding to $N = \pi/(a\epsilon)$ iterations. Hence the parameter values corresponding to the large N cycles approach the edge of the 0/1 stability interval as

$$\Omega(1/N) \approx \Omega_R + \pi^2/(aN)^2 \tag{7.8}$$

and the separation between the centres of the two consecutive stability intervals drops off as $2\pi^2/(a^2N^3)$. The entire stability intervals must be fitted into these gaps, so their widths must fall off at least as fast as $1/N^3$. As argued in section 2, for critical maps we furthermore expect the stability intervals and their neighborhoods to be self-similar, i.e. scale in the same way as the gaps. This agrees with the numerical evidence (7.5).

For every rational there is an infinity of harmonic sequences approximating it. We denote a member of such sequence by

$$(\omega, N, \tilde{\omega})_+ = \frac{(N + 1)P\tilde{Q} - P\tilde{Q}' - P'\tilde{Q}}{(N + 1)Q\tilde{Q} - Q\tilde{Q}' - Q'\tilde{Q}} \tag{7.9}$$

or

$$(\omega, N, \tilde{\omega})_- = \frac{(N - 1)P\tilde{Q} + P\tilde{Q}' + P'\tilde{Q}}{(N - 1)Q\tilde{Q} + Q\tilde{Q}' + Q'\tilde{Q}} \tag{7.10}$$

Here $\omega = P/Q$ is the limiting rational and $\omega = P'/Q'$ is its left parent. $\tilde{\omega} = \tilde{P}/\tilde{Q}$ is the tail of the continued fraction expansion (it labels the particular harmonic sequence), $\tilde{\omega}' = \tilde{P}'/\tilde{Q}'$ is its left parent, and N is the growing coefficient in the continued fraction expansion. + or – indicates that ω is being approached from above, resp. below. Furthermore, we define

$$(\omega, N, 1)_\pm = (\omega, N \mp 1, 0)_\pm \tag{7.11}$$

$$(1, N, \tilde{\omega})_\pm = 1 + (0, N \mp 1, \tilde{\omega})_\pm$$

The argument leading to (7.5) can be generalized to any harmonic sequence, leading to a cubic power law for the widths of the stability intervals:

$$N^3 \Delta(\omega, N, \tilde{\omega})_\pm \rightarrow \text{const.} \quad \text{as } N \rightarrow \infty \tag{7.12}$$

Our numerical results are in agreement with this estimate. For example, in Fig. 5 it can be seen that the expression (7.12) indeed approaches constant limit for various harmonic sequences. If we define $\delta(P/Q) = Q^3 \Delta(P/Q)$, this can be expressed as

$$\delta(\omega, N, \tilde{\omega})_\pm \rightarrow C_\pm(\omega, \tilde{\omega}), \quad \text{as } N \rightarrow \infty \tag{7.13}$$

The effect of the operators defined in the preceding section on a member of a harmonic sequence is as follows:

$$D(\omega, N, \tilde{\omega})_\pm = (\tilde{\omega}, N, \omega)_\pm \tag{7.14}$$

$$L(\omega, N, \tilde{\omega})_\pm = (\omega, N, T\tilde{\omega})_\pm, \quad \tilde{\omega} \neq 0, 1 \tag{7.15}$$

$$\omega, \quad \tilde{\omega} = 0$$

$$(\omega, N - 1, \tilde{\omega})_\pm, \quad \tilde{\omega} = 1$$

$$T(\omega, N, \tilde{\omega})_\pm = (T\omega, N, \tilde{\omega})_\pm, \quad \omega \neq 0, 1 \tag{7.16}$$

$$D\tilde{\omega}, \quad \omega = 0$$

$$(\omega, N - 1, \tilde{\omega})_\pm, \quad \omega = 1$$

Due to the symmetry between ω and $1 - \omega$ the width coefficients (7.13) satisfy

$$C_\pm(\omega, \tilde{\omega}) = C_\mp(1 - \omega, 1 - \tilde{\omega}) \tag{7.17}$$

8. Numerical results

We have computed the scaling functions (5.1) for the critical sine (1.1) and cubic (2.2) maps, and plotted them as functions of the (4.6), the dual of the daughter’s winding number

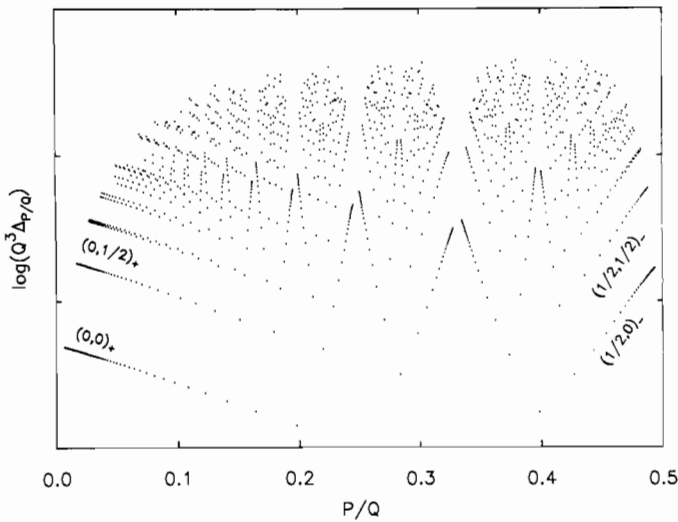


Fig. 5. Plot of $\log(Q^3 \Delta(P/Q))$. A few of the harmonic sequences are indicated.

$$\sigma(D\omega) = \frac{\Delta(\omega)}{\Delta(L\omega)} \quad (8.2)$$

or

$$\sigma(\omega) = \frac{\Delta(D\omega)}{\Delta(LD\omega)} = \frac{\Delta(D\omega)}{\Delta(DT\omega)}$$

The corresponding trivial scaling function (5.8) obeys a simple power law. For sine map (1.1) this scaling function is numerically almost smooth, as can be seen in Fig. 6. A striking feature of this scaling function is its “roof tiling” structure, which is still more apparent in the plot of $\sigma(x)/x^3$, Fig. 7, which shows that while different harmonic sequences do converge to 0_+ as expected from the cubic scaling for harmonic sequences (7.12), these limits are not universal.

From the arguments of the preceding section we know that the harmonic sequences have smooth left and right limits to each rational. However, different harmonic sequences have *different* limits: this is illustrated by Fig. 8 and Fig. 9, where we have plotted the values of the scaling function for 8

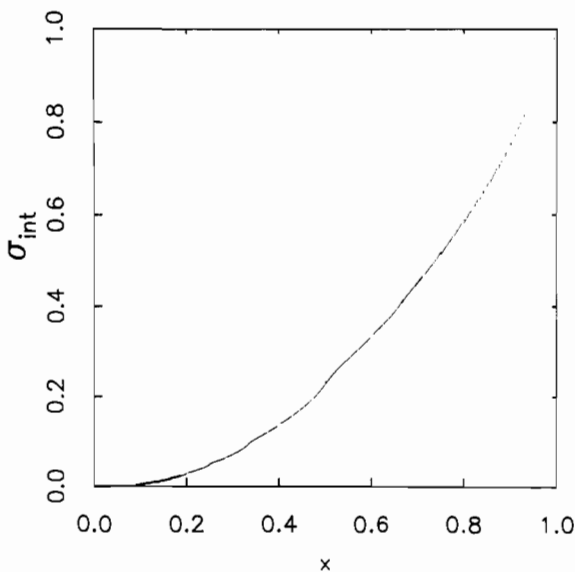


Fig. 6. The dual-labelled scaling function (8.2), plotted as a function of the ratio of daughter’s denominator with the left parent’s denominator.

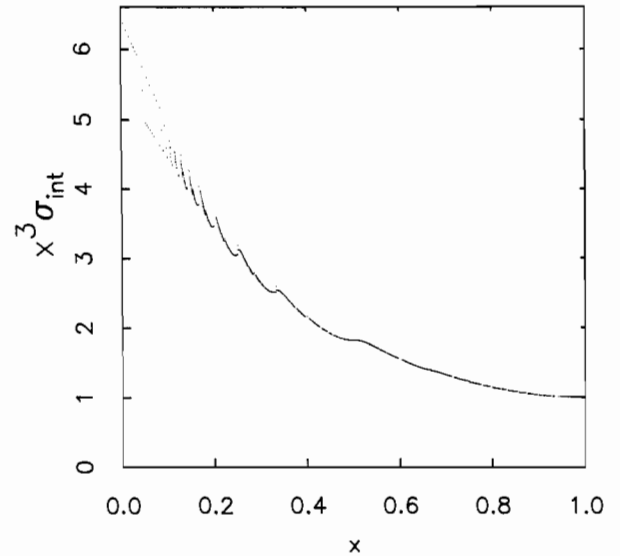


Fig. 7. Plot of $\sigma(x)/x^3$, a rescaled version of the scaling function of Fig. 6.

“Fibonacci” levels of harmonic sequences of type $(1, 1, \dots, N, 4) \rightarrow 1/4$. Harmonic sequences approximating any other rational have the same general structure:

1. The limit of an arbitrary harmonic sequence (for example, $[N, 4]$ in Fig. 8 or Fig. 9) is not universal: it depends on the particular circle map.
2. For a given daughter winding number and a given circle map, the values of the centroid (5.2), the interval (5.3) and the local (2.6) scaling functions are in general different.
3. The left and the right limits to a given rational are in general not the same, so the dual-labelled scaling functions (8.2) are *discontinuous* at every rational.
4. *Universal* scaling functions associated with the golden mean winding can be obtained by computing (8.2) only on the winding numbers $[1, 1, 1, \dots, 1, N, 1/x]$ sufficiently close to the golden mean. This follows from the existence of the unstable manifold for the circle maps [24], [25] and is illustrated by the harmonic sequences

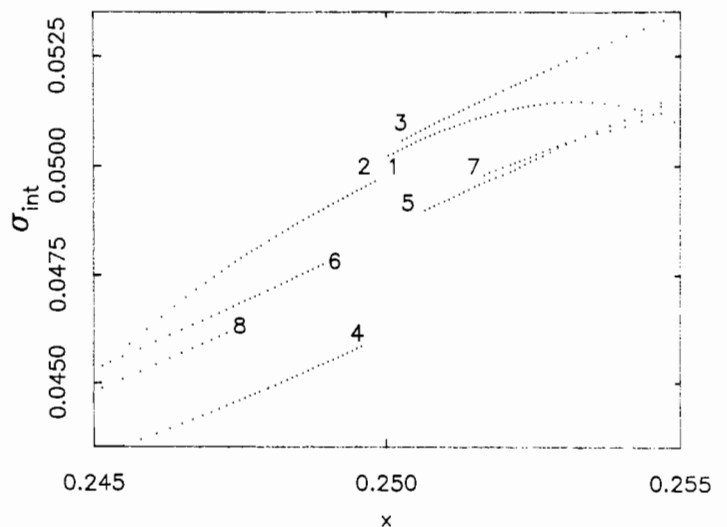


Fig. 8. The dual-labelled local (2.6) scaling function (8.2) for (1) $[N, 4]$, (2) $[1, N, 4]$, (3) $[1, 1, N, 4]$, (4) $[1, 1, 1, N, 4]$, etc., harmonic sequences evaluated for the cubic map (2.2).

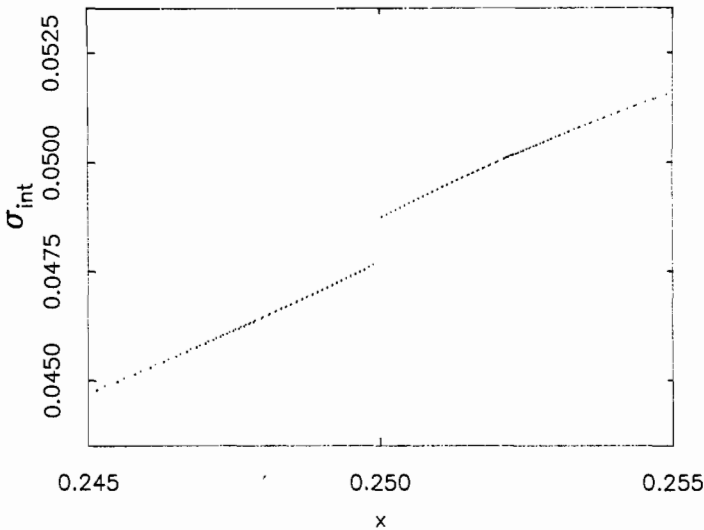


Fig. 9. The same as Fig. 8 evaluated for the sine map (1.1). The different sequences cannot be distinguished within the resolution of this plot. While the convergence is slower for the cubic map, both types of maps converge to the golden mean unstable manifold limit $[1, 1, \dots, 1, N, 4]$.

of Fig. 8. As can be seen by comparing Fig. 8 and Fig. 9, for the winding numbers close to the golden mean, the harmonic sequences limits for the cubic map and the sine map approach the same golden mean unstable manifold limit.

9. Summary

In this paper we have investigated numerically the scaling relations among mode lockings for circle maps. The mode lockings are naturally organized by Farey numbers, Fig. 1 to Fig. 3. Their scalings are summarized by the scaling functions of sections 6 and 8. We have constructed these scaling functions numerically from a large number of different sequences of mode lockings.

As these scaling functions apply to the entire range of winding numbers, they should be easier to observe experimentally than the universality for the golden mean winding number, the special case of the above theory. It should be possible to check much of the circle map scaling structure, provided sufficiently many mode-locking intervals can be measured.

In our investigations we have concentrated on the scalings in parameter space. However, it is clear that the self-similarity relations also extend to the iteration space [26], and that the more general scaling laws will have structure reminiscent of the unstable manifold equations [3], [27], [28], i.e., be formulated in terms of simultaneous shifts and rescalings in both parameter and iteration spaces.

Finally, we expect the methods of this paper to have theoretical implications beyond their application to just circle maps. There is a number of other physical problems which exhibit mode-locking, and are presumably amenable to organization by the Farey trees. *Hamiltonian* mappings are one class of such problems. Another problem with universality organized

by Farey trees are the universal scaling laws for *complex* iterations [28–32].

Acknowledgements

We are grateful to P. Grassberger, M. H. Jensen, J. Myrheim, S. Ostlund, T. Bohr and M. J. Feigenbaum for many inspiring discussions. P.C. thanks C. Pethick for kind hospitality in his tent in Greenland, in which a significant part of this work was done. The bulk of the work was done at Nordita. P.C. acknowledges support from DOE contract no. DE-ACO2-83-ER13044.

References

1. Feigenbaum, M. J., *J. Stat. Phys.* **19**, 25 (1978).
2. Feigenbaum, M. J., *J. Stat. Phys.* **21**, 669 (1979), reprinted in ref. [3].
3. Cvitanović, P., ed., *Universality in chaos* (Hilger, Bristol, 1984).
4. Collet, P. and Eckmann, J.-P., *Iterated maps on interval as dynamical systems* (Birkhauser, Boston, 1980).
5. Cvitanović, P., *Acta Phys. Pol.* **A65**, 203 (1984), reprinted in ref. [3].
6. Eckmann, J.-P., *Rev. Mod. Phys.* **53**, 643 (1981), reprinted in ref. [3].
7. Hu, B., *Phys. Rep.* **91**, 233 (1982).
8. Jensen, M. H., Bak, P. and Bohr, T., *Phys. Rev.* **A30**, 1960 (1984).
9. Bohr, T., Jensen, M. H. and Bak, P., *Phys. Rev.* **A30**, 1970 (1984).
10. Shenker, S. J., *Physica* **5D**, 405 (1982), reprinted in ref. [3].
11. Feigenbaum, M. J., Kadanoff, L. P. and Shenker, S. J., *Physica* **5D**, 370 (1982).
12. Ostlund, S., Rand, D., Sethna, J. and Siggia, E. D., *Physica* **D8**, 303 (1983).
13. Jensen, M. H., Bak, P. and Bohr, T., *Phys. Rev. Lett.* **50**, 1637 (1983).
14. Myrheim, J., unpublished.
15. This has been observed by Gonzales, D. L. and Piro, O., *Phys. Rev. Lett.* **50**, 870 (1983), and probably by many other authors.
16. See, for example, Ostlund, S. and Kim, S.-h., *Phys. Scripta*, T9, 193 (1985), for related applications of Farey numbers.
17. Hardy, G. H. and Wright, E. M., *Theory of numbers* (Oxford Univ. Press, Oxford, 1938).
18. Allen, T., *Physica* **6D**, 305 (1983).
19. We are indebted to J. Myrheim for this observation.
20. P. Grassberger has also introduced this binary labelling of Farey trees (unpublished).
21. Feigenbaum, M. J., Cornell preprint, March 1984.
22. Cvitanović, P., unpublished.
23. Pomeau, Y. and Manneville, P., *Commun. Math. Phys.* **74**, 189 (1980).
24. Feigenbaum, M. J. and Gunratne, G., unpublished.
25. Cvitanović, P., Jensen, M. H., Kadanoff, L. P. and Procaccia, I., *Phys. Rev. Lett.*, to appear.
26. Farmer, J. D. and Satija, I., *Phys. Rev. A* (May 1985).
27. Golberg, A. I., Sinai, Ya. G. and Khanin, K. M., *Usp. Mat. Nauk* **38**, 159 (1983).
28. Cvitanović, P. and Myrheim, J., Nordita preprint 84/5 (1984), submitted to *Comm. Math. Phys.* ages ago.
29. Golberg, A. I., Sinai, Ya.G. and Khanin, K. M., *Usp. Mat. Nauk* **38**, 159 (1983).
30. Cvitanović, P. and Myrheim, J., *Phys. Lett.* **94A**, 329 (1983).
31. Manton, N. S. and Nauenberg, M., *Commun. Math. Phys.* **89**, 555 (1983).
32. Widom, M., *Commun. Math. Phys.* **92**, 121 (1983).